Report Documentation Page

Form Approved
OMB No. 0704-0188

1. REPORT DATE	2. REPORT TYPE	3. DATES COVERED
23 OCT 2012		**00-00-2012 to 00-00-2012**

4. TITLE AND SUBTITLE	5a. CONTRACT NUMBER
Optically pumped coherent mechanical oscillators:the laser rate equation theory and experimental verification	5b. GRANT NUMBER
	5c. PROGRAM ELEMENT NUMBER
6. AUTHOR(S)	5d. PROJECT NUMBER
	5e. TASK NUMBER
	5f. WORK UNIT NUMBER
7. PERFORMING ORGANIZATION NAME(S) AND ADDRESS(ES) **Naval Research Laboratory,Washington,DC,20375**	8. PERFORMING ORGANIZATION REPORT NUMBER
9. SPONSORING/MONITORING AGENCY NAME(S) AND ADDRESS(ES)	10. SPONSOR/MONITOR'S ACRONYM(S)
	11. SPONSOR/MONITOR'S REPORT NUMBER(S)

12. DISTRIBUTION/AVAILABILITY STATEMENT
Approved for public release; distribution unlimited

13. SUPPLEMENTARY NOTES
New Journal of Physics 14 (2012)

14. ABSTRACT

15. SUBJECT TERMS

16. SECURITY CLASSIFICATION OF:			17. LIMITATION OF ABSTRACT	18. NUMBER OF PAGES	19a. NAME OF RESPONSIBLE PERSON
a. REPORT **unclassified**	b. ABSTRACT **unclassified**	c. THIS PAGE **unclassified**	**Same as Report (SAR)**	**17**	

New Journal of Physics
The open-access journal for physics

Optically pumped coherent mechanical oscillators: the laser rate equation theory and experimental verification

J B Khurgin[1], M W Pruessner[2,3], T H Stievater[2] and W S Rabinovich[2]

[1] Department of Electrical and Computer Engineering, Johns Hopkins University, Baltimore, MD 21218, USA
[2] Naval Research Laboratory, Washington, DC 20375, USA
E-mail: marcel.pruessner@nrl.navy.mil

New Journal of Physics **14** (2012) 105022 (15pp)
Received 21 May 2012
Published 23 October 2012
Online at http://www.njp.org/
doi:10.1088/1367-2630/14/10/105022

Abstract. We develop a theory describing the operation of an opto-mechanical oscillator as a phonon laser using a set of coupled equations that is analogous to the standard set of laser rate equations. We show that laser-like parameters that characterize gain, stored energy, threshold, efficiency, oscillation frequency linewidth, and saturation power can be introduced for an opto-mechanical oscillator driven by photo-thermal or radiation pressure forces. We then apply the theoretical model to the experimental results for photo-thermally driven oscillations in a Si waveguide opto-mechanical resonator and show good agreement between the theory and experiments. We also consider the microscopic mechanism that transforms the energy of incoherent thermal phonons into coherent oscillations of a single phonon mode and show remarkable parallels with the three-wave parametric interactions in optics and also with opto-electronic oscillators used in microwave photonics.

[3] Author to whom any correspondence should be addressed.

Contents

1. Introduction 2
2. Experiment 3
3. Derivation of rate equations 4
4. Rate equation solution and comparison with experiment 11
5. Microscopic picture 13
6. Conclusions 14
References 15

1. Introduction

Advances made in the last decade in the field of micro-fabrication have created a number of new fields in physics and optics, including cavity opto-mechanics. Cavity opto-mechanics enables resonantly enhanced light to exert forces on small mechanical objects with high-quality mechanical (acoustic) resonances [1–3]. These forces can be of a direct nature, such as the force caused by the momentum of light (i.e. radiation pressure), or more involved, mediated by the heating of the mechanical object (i.e. photothermal force). A feedback mechanism is established when the mechanical object comprises either the whole resonant cavity (as in micro-discs and toroids [4]) or a part of it (as in various Fabry–Perot cavities [5]). Tuning the optical wavelength around the resonance enables external optical control of both the frequency and amplitude of the mechanical oscillations—a feature that can be used in various practical applications, particularly in sensing. From a practical point of view, the control of amplitude has been the main focus of attention of many groups, and it is quite remarkable that by changing the sign of the detuning one can either decrease or increase the vibration amplitude of a mechanical mode, which can be construed as 'cooling' [6–8] or 'amplifying' [9–12] this mode, respectively. Achieving opto-mechanical cooling has been the goal of most researchers [6–8], since an optically cooled mechanical mode enables access to the quantum regime of a mechanical resonator [13]. However, the opposite effect (i.e. the resonant amplification of a mechanical mode) can be exploited in high sensitivity detection. A large increase in the amplitude of mechanical oscillations with optical power is always accompanied by a reduction of the linewidth of these oscillations. Consequently, minute changes in, e.g., the mass of the oscillating mechanical object due to attached particles, or the strain due to changes in pressure, will induce a commensurate change in the resonant frequency. This frequency shift can be detected with great precision by simply monitoring the light emerging from the opto-mechanical resonator whose motion has now amplitude modulated the optical signal.

This effect of sharp narrowing of the linewidth of opto-mechanical oscillation is the main focus of this work and we shall show that this narrowing can be treated in a manner similar to the narrowing of the linewidth occurring in lasers operating above threshold. Indeed, it has been shown in various opto-mechanical schemes that beyond a certain threshold power, self-sustained mechanical oscillations materialize [9, 10], causing a number of researchers to claim mechanical or phonon lasing [11, 12]. In the optical domain the sharp rise in amplitude of oscillations and simultaneous linewidth collapse are two telltale signs usually accepted as unequivocal proof of lasing. Since mechanical oscillations are in essence vibrations of phonon modes, it is reasonable to depict the above-threshold opto-mechanical oscillation as phonon lasing. However, at this

time the framework in which the 'phonon lasers' are described is different from the traditional laser theory in which such key parameters as 'gain', 'population inversion' and 'saturation' are prominently featured. Lasing is typically described by a set of two coupled rate (balance) equations: one for the gain (or population inversion) and the other for the bosons in the resonant mode [14–16] and no equivalent set of equations has been developed for the opto-mechanical oscillations. Generation of coherent photons and of coherent phonons, two processes that are described virtually identically on the quantum level, are treated within two entirely different frameworks. It is precisely the goal of this work to bridge the concepts of laser physics and opto-mechanical oscillators and to bring these two communities together.

In this paper, we review our initial experimental work [17] on optically pumped micro-mechanical oscillators. We expand our recently developed opto-mechanical rate equation theory, which was only briefly introduced in [18]; this allows us to describe the dynamics of an optically driven micro-mechanical oscillator in terms of gain, stored energy, slope efficiency and saturation power. In this picture, the driven mechanical oscillator behaves much like a laser in which pump photons generate coherent acoustic phonons. Our theory is verified by experiments that show a threshold behavior beyond which the mechanical resonance linewidth collapses and the oscillation amplitude increases sharply. We conclude with an analysis of the device behavior at the quantum level, in which the population inversion required for optical lasers now consists of high-frequency phonon pairs whose phase coherence enables phonon 'lasing' and discuss parallels with the three-wave parametric interactions in optics and with opto-electronic oscillators used in microwave photonics.

2. Experiment

The opto-mechanical oscillator [17] we consider is shown in figure 1. It consists of a waveguide Fabry–Perot microcavity with two sets of silicon/air gratings as mirrors fabricated from a silicon-on-insulator wafer. One of the gratings is movable and attached to the center of a silicon microbridge whose buried SiO_2 layer has been etched away to leave a suspended beam anchored only at its ends. As the bridge oscillates (e.g. due to thermal fluctuations) the mirror is displaced and the Fabry–Perot cavity is tuned. For a fixed input laser wavelength and power, the cavity tuning implies a modulation of transmitted output power corresponding to the mirror/bridge motion.

For high-Q_{optical} cavities there can be a large instantaneous circulating power inside the cavity when the laser wavelength is tuned close to the cavity optical resonance. Any optical forces are then amplified so that they can have a significant effect on the mirror/bridge motion. Feedback is achieved since the optical force implies a subsequent change in mirror position with a resulting cavity tuning. For a fixed laser wavelength the cavity tuning results in a change in circulating cavity power and a change in the optical force exerted on the mirror/bridge.

In our device both radiation pressure and photothermal forces exist. However, there is a large difference in force time constants—radiation pressure is governed by the short (fast) cavity photon lifetime, while photothermal forces are dictated by the device's long (slow) thermal time constant [17]. The result is that optical force-induced frequency tuning of the mechanical oscillator is governed by radiation pressure, while damping (cooling) and amplification of the oscillator motion is dominated by photothermal forces. As we will show below, self-oscillation in our device is dominated by photothermal forces.

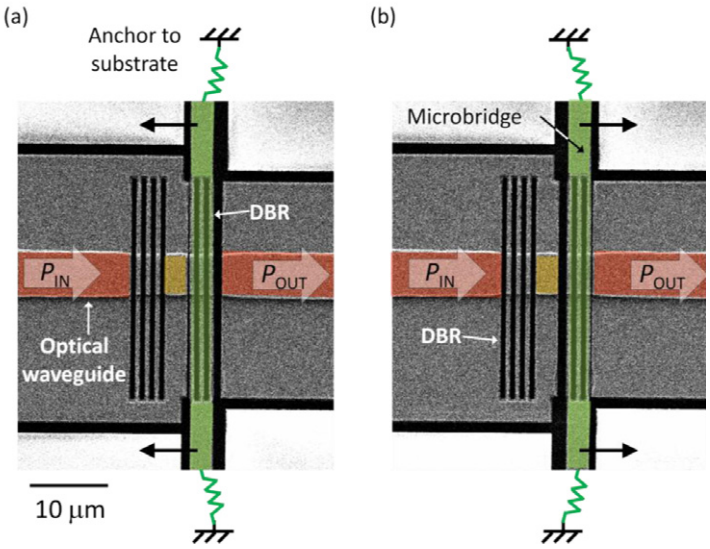

Figure 1. (a, b) Schematic diagram of the fabricated device showing the micromechanical oscillator (green) and the waveguide optical Fabry–Perot cavity with silicon/air gratings (red/orange). The images were taken by a scanning electron microscope in which charging leads to electrostatic self-actuation of the microbridge (green). In this work, the actual mirror displacement due to optical forces will be much smaller.

Since our opto-mechanical device architecture is fully integrated, the measurements are made using a relatively simple setup shown in figure 2. The device is placed in a vacuum cell with sapphire windows and all experiments are performed at room temperature and $\sim$20 mTorr pressure. Further experimental details can be found in [17]. Figure 3 shows a set of measurements exhibiting the well-known opto-mechanical instability in which self-oscillation occurs once the optical power crosses a threshold value; in our experiments the threshold power is around 300 μW (device 1). We emphasize that in contrast to radiation pressure-based opto-mechanical instability occurring for a blue-detuned laser (e.g. [7]), our device exhibits self-oscillation for a red-detuned laser. The reason for the change in the required detuning has to do with the unique device architecture. While radiation pressure always displaces a mirror in the positive direction (i.e. to lengthen the Fabry–Perot cavity as in figure 1(b)), the photothermal force can act in either the positive or the negative direction. In our case, photothermal effects result in local heating that displaces the movable mirror to shorten the Fabry–Perot cavity (i.e. in the negative direction as in figure 1(a)) [17].

3. Derivation of rate equations

The 'lasing' process follows the cycle shown in figure 4 and is based on photothermal forces (we note that a similar lasing process occurs for radiation pressure-based devices). The DBR mirror and microbridge oscillate, initially due to thermal fluctuations. This causes the optical power circulating inside the cavity to be modulated in proportion to the oscillations. A fraction of the optical power is absorbed by the distributed Bragg reflector (DBR) mirror [17], resulting in local

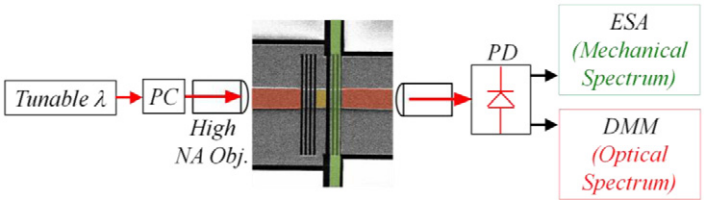

Figure 2. The experimental setup: continuous wave (CW) light from a tunable laser is sent to the device using a high-numerical aperture (NA) objective (PC: polarization controller); the device optical response is similarly collected and the modulated signal is measured in a photodetector (PD). The optical resonance spectrum is measured using a digital multi-meter (DMM) by sweeping the laser wavelength. The mechanical resonance is obtained by fixing the laser wavelength and measuring the modulated optical signal in an electrical spectrum analyzer (ESA). For all measurements the device is kept in vacuum (∼20 mTorr).

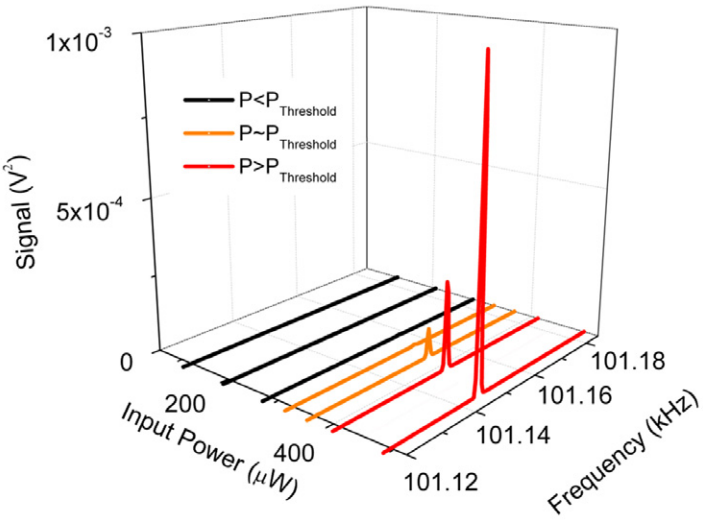

Figure 3. Measured mechanical resonance spectrum for different optical powers (device 1). The laser wavelength is red-detuned with respect to the cavity optical resonance. We measure a clear threshold power beyond which the oscillation amplitude increases sharply and the mechanical linewidth collapses (linewidth was deconvolved from ESA filter response).

heating, thermal expansion and an effective photothermal force. The optical force changes the microbridge displacement and the process repeats itself.

We now offer a detailed derivation of a set of two opto-mechanical laser rate equations. Since the 'output power' of a mechanical laser is related to the vibration amplitude and the gain to the temperature rise (for a photothermal force), it is the equations for these two variables that serve as a basis for our derivations. The position of the beam has both steady state and oscillating components,

$$\Delta z = \Delta\bar{z} + z_{\mathrm{m}}\cos(\omega t) = \Delta\bar{z} + \tfrac{1}{2}z_{\mathrm{m}}\exp(\mathrm{j}\omega t) + \mathrm{c.c.}, \tag{1}$$

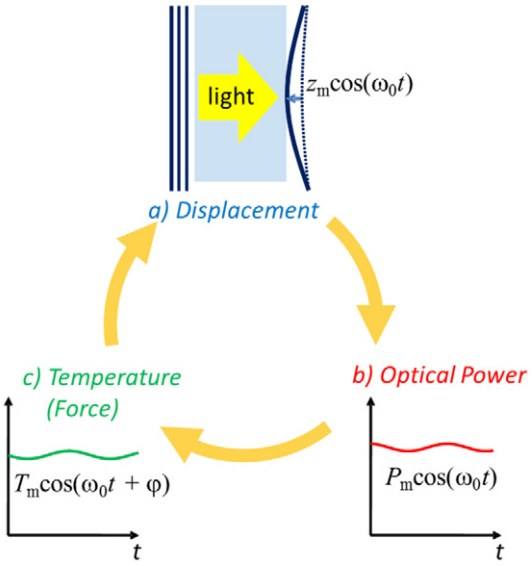

Figure 4. The lasing cycle in the photo-thermal oscillator: oscillating mechanical mode (a) modulates the optical power in the cavity (b), causing a temperature change and a resulting force (c). This force causes the microbridge to be displaced (a) and the cycle repeats itself.

where ω is the resonant frequency of the beam modified by the optical force, $\Delta\bar{z}$ is the steady-state shift of the beam position relative to its position in the absence of light, and z_m is the slow-variable amplitude (i.e. $dz_m/dt \ll \omega$). Note that we choose the initial phase of oscillation to be 0 which makes z_m real and simplifies the derivations. A change in the optical cavity length causes a change in the optical power P at the DBR etched into the microbridge. This power also has two components,

$$\Delta P = \Delta\bar{P} + \tfrac{1}{2}P_m \exp(j\omega t) + \text{c.c.}, \tag{2}$$

which causes the temperature of the mechanical oscillator to rise relative to the ambient temperature

$$\Delta T = \Delta\bar{T} + \tfrac{1}{2}T_m \exp(j\omega t) + \text{c.c.} \tag{3}$$

The temperature rise can be determined by substituting (2) and (3) into the equation

$$\frac{dT}{dt} = \frac{\alpha R_t P}{\tau_t} - \frac{T}{\tau_t}, \tag{4}$$

where α is the total absorption in the beam, R_t is the thermal resistance and τ_t is the thermal relaxation time. This yields

$$\begin{aligned} \Delta\bar{T} &= \alpha R_t \Delta\bar{P}, \\ dT_m/dt &= -(j\omega - 1/\tau_t)T_m + \alpha R_t P_m/\tau_t, \end{aligned} \tag{5}$$

with the delay τ_t indicating that temperature oscillations are shifted in phase relative to the optical power and thus their amplitude T_m is complex.

The relation between the displacement and the power on the DBR is determined by the resonance characteristics of the Fabry–Perot cavity incorporating the DBR and characterized

by the finesse F, quality factor $Q_{\rm opt}$ and cavity transmission at the resonance $T_{\rm cav}$, which in our experiments was significantly less than unity due to scattering at the air gaps in the DBR. When $c/\lambda Q_{\rm opt} \gg \omega$ the power at the DBR follows the DBR displacement adiabatically, and can be given as

$$P(\Delta z) = \frac{\frac{2}{\pi n_{\rm Si}} F T_{\rm cav}^{1/2}}{1 + \left(\frac{2}{\pi} F \sin \pi \frac{2(l_{\rm opt}+\Delta z)}{\lambda}\right)^2} P_{\rm in}(t), \tag{6}$$

where $P_{\rm in}(t)$ is the slowly variable waveguide optical power incident on the cavity and $l_{\rm opt}$ is the optical length of the cavity. When the cavity is at the exact resonance $l_{\rm opt} = N\lambda/2$, the power inside it is at a maximum, the derivative over the DBR displacement is equal to zero and there is no feedback between the mechanical oscillations and optical force causing them. To optimize that feedback, i.e. to maximize the derivative $\mathrm{d}P/\mathrm{d}z$, the resonator should be detuned by a small amount, $\Delta\lambda \approx \mp\lambda/(2\sqrt{3}Q_{\rm opt})$. This causes the second derivative $\mathrm{d}^2P/\mathrm{d}z^2$ to vanish and only the first and third-order derivatives may be kept in a series expansion of power

$$P(\Delta z - \Delta\bar{z}) = P(l_{\rm opt} + \Delta\bar{z}) + \left.\frac{\mathrm{d}P}{\mathrm{d}z}\right|_{l_{\rm opt}+\Delta\bar{z}} (\Delta z - \Delta\bar{z}) + \frac{1}{6}\left.\frac{\mathrm{d}^3P}{\mathrm{d}z^3}\right|_{l_{\rm opt}+\Delta\bar{z}} (\Delta z - \Delta\bar{z})^3, \tag{7}$$

where

$$\begin{aligned} \frac{\mathrm{d}P}{\mathrm{d}z} &= z_1^{-1} P_{\rm in} \approx \mp(3F)^2/(\pi n_{\rm Si}\sqrt{3}) T_{\rm cav}^{1/2} \lambda^{-1} P_{\rm in}, \\ \frac{\mathrm{d}^3P}{\mathrm{d}z^3} &= z_3^{-3} P_{\rm in} \approx \pm 8\,(3F)^4/(\pi\sqrt{3}) T_{\rm cav}^{1/2} \lambda^{-3} n_{\rm Si}^{-3} P_{\rm in}. \end{aligned} \tag{8}$$

The change of sign corresponds to the red and blue shifts of the wavelengths, the first-order term describes the strength of the feedback exerted by the DBR displacement onto the optical force, and the third-order term (which always has an opposite sign) describes the saturation. If one introduces the saturation amplitude as $z_{\rm sat} = \sqrt{-z_3^3/z_1} \approx \lambda n_{\rm Si}/3F$ and then substitutes (1) into (7), one arrives at the relation

$$P_{\rm m}(t) = P_{\rm in}(t) \frac{z_{\rm m}}{z_1} \left(1 - \frac{z_{\rm m}^2}{z_{\rm sat}^2}\right). \tag{9}$$

In figure 5, we have plotted the exact value of the derivative $\mathrm{d}P/\mathrm{d}z$ as a function of DBR displacement as well as its parabolic approximation. Clearly, the saturation amplitude $z_{\rm sat}$ defines the range of sustainable opto-mechanical oscillations.

Substituting (9) into (5), we obtain the relation between the amplitudes of temperature rise and DBR displacement

$$\frac{\mathrm{d}T_{\rm m}(t)}{\mathrm{d}t} + \mathrm{j}\omega T_{\rm m}(t) + \frac{T_{\rm m}(t)}{\tau_{\rm t}} = \frac{\alpha R_{\rm t}}{\tau_{\rm t}} P_{\rm in}(t) \frac{z_{\rm m}}{z_1} \left[1 - \frac{z_{\rm m}^2}{z_{\rm sat}^2}\right]. \tag{10}$$

Splitting the temperature rise into in-phase (real: T') and quadrature (imaginary: T'') components yields

$$\begin{aligned} \frac{\mathrm{d}T'_{\rm m}(t)}{\mathrm{d}t} - \omega T''_{\rm m}(t) + \frac{T'_{\rm m}(t)}{\tau_{\rm t}} &= \frac{\alpha R_{\rm t}}{\tau_{\rm t}} P_{\rm in}(t) \frac{z_{\rm m}}{z_1} \left[1 - \frac{z_{\rm m}^2}{z_{\rm sat}^2}\right], \\ \frac{\mathrm{d}T''_{\rm m}(t)}{\mathrm{d}t} + \omega T'_{\rm m}(t) + \frac{T''_{\rm m}(t)}{\tau_{\rm t}} &= 0. \end{aligned} \tag{11}$$

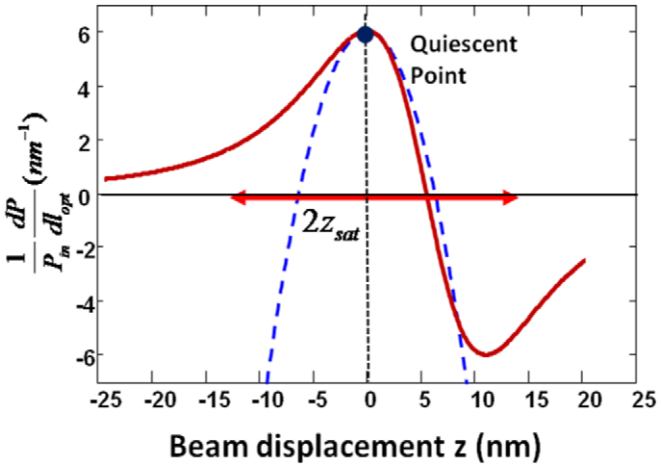

Figure 5. Change in cavity optical power as a function of reflector position and its lowest-order series expansion (dashed line) with the quiescent point for optimal device operation and the saturation amplitude, z_{sat}, listed.

Working in our slowly varying approximation framework $\mathrm{d}/\mathrm{d}t \ll \omega,\ \tau_{\mathrm{t}}^{-1}$, we can drop the derivative term in the second equation and assume that the quadrature component of temperature oscillations follows the real component adiabatically as $T''_{\mathrm{m}}(t) = -\omega\tau_{\mathrm{t}}T'_{\mathrm{m}}(t)$ and obtain by substitution into the first of equations (11)

$$\begin{aligned}\frac{\mathrm{d}T'_{\mathrm{m}}(t)}{\mathrm{d}t} + \frac{T'_{\mathrm{m}}(t)}{\tau_{\mathrm{t}}}\left(1+\omega^2\tau_{\mathrm{t}}^2\right) &= \frac{1}{\tau_{\mathrm{t}}}\alpha R_{\mathrm{t}} P_{\mathrm{in}}(t)\frac{z_{\mathrm{m}}}{z_1}\left[1-\frac{z_{\mathrm{m}}^2}{z_{\mathrm{sat}}^2}\right],\\ \frac{\mathrm{d}T''_{\mathrm{m}}(t)}{\mathrm{d}t} + \frac{T''_{\mathrm{m}}(t)}{\tau_{\mathrm{t}}}\left(1+\omega^2\tau_{\mathrm{t}}^2\right) &= -\omega\alpha R_{\mathrm{t}} P_{\mathrm{in}}(t)\frac{z_{\mathrm{m}}}{z_1}\left[1-\frac{z_{\mathrm{m}}^2}{z_{\mathrm{sat}}^2}\right].\end{aligned} \tag{12}$$

Now that we have determined how the amplitude and phase temperature oscillations relate to the mechanical oscillations, we need to determine the feedback process that causes a change in the amplitude and phase of mechanical oscillations because of the oscillations in temperature. The equation governing the displacement of the beam $\Delta z(\mathrm{t})$ is that of a damped harmonic oscillator

$$\frac{\mathrm{d}^2\Delta z}{\mathrm{d}t^2} + \gamma\frac{\mathrm{d}\Delta z}{\mathrm{d}t} = -\omega_0^2\left[\Delta z(t) - \Delta z_0(t)\right], \tag{13}$$

whose 'instant equilibrium' position (i.e. the position to which the elastic force is trying to return at a given instant) depends on the temperature as

$$\Delta z_0(t) = -\frac{\mathrm{d}z}{\mathrm{d}T}T(t), \tag{14}$$

where $-\partial z/\partial T$ is a thermal-displacement gain coefficient that relates the beam displacement to changes in temperature via thermal expansion [17]. Using (3) we obtain

$$\Delta z_0(t) = -\frac{\mathrm{d}z}{\mathrm{d}T}\Delta\bar{T} - \frac{1}{2}\frac{\mathrm{d}z}{\mathrm{d}T}\left[T_{\mathrm{m}}\exp\left(\mathrm{j}\omega t\right) + \mathrm{c.c.}\right]. \tag{15}$$

Inserting (1) and (15) into (13), equating the terms with the same harmonic dependence, and neglecting the second-order derivative of slowly varying amplitude z_m and another small

term $\gamma\, \mathrm{d}z_\mathrm{m}/\mathrm{d}t$, we obtain

$$\frac{\mathrm{d}z_\mathrm{m}}{\mathrm{d}t} = -\frac{\gamma}{2} z_\mathrm{m} - \frac{\mathrm{j}}{2\omega}\left(\omega^2 - \omega_0^2 - \omega_0^2 \frac{\mathrm{d}z}{\mathrm{d}T}\frac{T'_\mathrm{m}}{z_\mathrm{m}}\right) z_\mathrm{m} - \frac{1}{2\omega}\omega_0^2 \frac{\mathrm{d}z}{\mathrm{d}T} T''_\mathrm{m}. \tag{16}$$

The first term describes the damping; since z_m is real, the term in parentheses must be equal to zero, indicating an observed resonant frequency shift [17, 19]

$$\omega^2 = \omega_0^2 + \omega_0^2 \frac{\mathrm{d}z}{\mathrm{d}T}\frac{T'_m}{z_m}, \tag{17}$$

that can also be thought of as frequency pulling in a conventional laser theory ([14], equations (12) and (13)). The last term, which can be modified by dividing and multiplying by z_m, describes the gain, i.e. the equation can be written as

$$\frac{\mathrm{d}z_\mathrm{m}}{\mathrm{d}t} = \frac{1}{2}\left(g(t) - \gamma\right) z_\mathrm{m}, \tag{18}$$

where we have introduced our gain (per unit of time) as

$$g = -(\omega_0^2/\omega)(\mathrm{d}z/\mathrm{d}T) T''_\mathrm{m}/z_\mathrm{m}. \tag{19}$$

Note that just the quadrature component of T_m contributes to the gain, which is precisely the 90° phase shift occurring in optical parametric oscillators [14]—an analogy explored below. Finally, from (18), we obtain for the square of the amplitude

$$\frac{\mathrm{d}z_\mathrm{m}^2}{\mathrm{d}t} = [g(t) - \gamma] z_\mathrm{m}^2. \tag{20}$$

The rate equation for the gain is then obtained from the second equation in (12) as

$$\frac{\mathrm{d}g}{\mathrm{d}t} + \frac{g}{\tau'_\mathrm{t}} = \frac{g_0}{\tau'_\mathrm{t}}\left(1 - z_\mathrm{m}^2/z_\mathrm{sat}^2\right), \tag{21}$$

where the unsaturated gain is $g_0(P_\mathrm{in}) = \alpha\, (\mathrm{d}z/\mathrm{d}T)\, R_\mathrm{t} P_\mathrm{in}(t) z_1^{-1} \omega^2 \tau'_\mathrm{t}$, and the modified thermal relaxation time is $\tau'_\mathrm{t} = \tau_\mathrm{t}/(1 + \omega^2 \tau_\mathrm{t}^2)$. Equations (20) and (21) represent our main result: a coupled set of equations for gain and oscillating power (oscillation amplitude) in an opto-mechanical system.

We rewrite equations (20) and (21) as a set of standard laser rate equations (equation 13.43 in [14]) to better describe the energy balance. The energy of mechanical vibrations is $U_\mathrm{m} = \frac{1}{2} m_\mathrm{eff} \omega^2 z_\mathrm{m}^2$, its saturation value is defined as $U_\mathrm{sat} = \frac{1}{2} m_\mathrm{eff} \omega^2 z_\mathrm{sat}^2$, where m_eff is the effective mass of the beam, and another variable, the stored energy of phase-locked thermal phonons that are available for 'lasing', is given by $U_\mathrm{st} = g \tau'_\mathrm{t} U_\mathrm{sat}$, whose unsaturated value is $U_{\mathrm{st},0} = g_0 \tau'_\mathrm{t} U_\mathrm{sat}$. We also include the thermal noise power $P_\mathrm{N} = \gamma k T/2$ in the equation to obtain

$$\begin{aligned} \frac{\mathrm{d}U_\mathrm{st}}{\mathrm{d}t} &= \frac{U_{\mathrm{st},0}}{\tau'_\mathrm{t}}\left[1 - \frac{U_\mathrm{m}}{U_\mathrm{sat}}\right] - \frac{U_\mathrm{st}}{\tau'_\mathrm{t}}, \\ \frac{\mathrm{d}U_\mathrm{m}}{\mathrm{d}t} &= \left[\frac{U_\mathrm{st}}{\tau'_\mathrm{t} U_\mathrm{sat}} - \gamma\right] U_\mathrm{m} + P_\mathrm{N}. \end{aligned} \tag{22}$$

For the relatively weak vibrations ($z_m \ll z_{\rm sat}$), equation (22) can be approximated as

$$\begin{aligned}\frac{{\rm d}U_{\rm st}}{{\rm d}t} &= \eta_{\rm p} P_{\rm in} - \frac{U_{\rm st}}{\tau_{\rm t}'} - \frac{U_{\rm st}}{\tau_{\rm t}'}\frac{U_{\rm m}}{U_{\rm sat}},\\ \frac{{\rm d}U_{\rm m}}{{\rm d}t} &= \frac{U_{\rm st}}{\tau_{\rm t}' U_{\rm sat}} U_{\rm m} - \gamma U_{\rm m} + P_N,\end{aligned} \tag{23}$$

where we have introduced the pumping efficiency

$$\eta_{\rm p} = \frac{U_{\rm st,0}}{P_{\rm in}\tau_{\rm t}'} = \frac{\omega T_{\rm cav}^{1/2}}{2\pi\sqrt{3}}\alpha R_{\rm t}\frac{{\rm d}z}{{\rm d}T} K_{\rm eff}\lambda n_{\rm Si}\omega\tau_{\rm t}', \tag{24}$$

and $K_{\rm eff} = m_{\rm eff}\omega_0^2$ is the effective spring coefficient. The stimulated emission term $U_{\rm st}U_{\rm m}/U_{\rm sat}\tau_{\rm t}'$ appears in both equations for stored and released energies with opposite signs indicating perfect energy balance as the energy is transferred from thermal phonons in all acoustic modes into coherent phonons in a single resonant mechanical mode. Also, note that neither $U_{\rm st,0}$ nor $\eta_{\rm p}$ depends on cavity finesse, which is consistent because they basically represent the area under the optical force curve in figure 5.

Next, we divide all the energies by a phonon energy $\hbar\omega$ to obtain a standard set of the Statz–de-Mars [15, 16] balance equations

$$\begin{aligned}\frac{{\rm d}N_{\rm st}}{{\rm d}t} &= \frac{N_{\rm st,0}}{\tau_{\rm t}'} - \frac{N_{\rm st}}{\tau_{\rm t}'}\left[1 + \frac{n_{\rm m}}{N_{\rm sat}}\right],\\ \frac{{\rm d}n_{\rm m}}{{\rm d}t} &= \left[\frac{N_{\rm st}}{\tau_{\rm t}' N_{\rm sat}} - \gamma\right] n_{\rm m} + \gamma\frac{kT}{2\hbar\omega},\end{aligned} \tag{25}$$

with $n_{\rm m}$ being the number of coherent phonons, $N_{\rm st}$ playing the role of population inversion and $(\tau_{\rm t}' N_{\rm sat})^{-1}$ being the equivalent of the stimulated emission coefficient. One difference between rate equations (25) and the standard laser equations is that the noise term is of thermal nature and thus appears to be classical. However, this is simply the approximation of a fully quantum Bose–Einstein distribution term for the case of $kT \gg \hbar\omega$ and is not related to the fact that our quanta are phonons and not photons.

Finally, let us introduce the threshold value of stored energy, $U_{\rm st,th} = \gamma\tau_{\rm t}' U_{\rm sat}$, and the threshold pump power

$$P_{\rm th} = U_{\rm st,th}/\eta_{\rm p}\tau_{\rm t}' \approx \frac{0.62}{Q_{\rm m}F^2 T_{\rm cav}^{1/2}}\frac{1+\omega^2\tau_{\rm t}^2}{\omega\tau_{\rm t}}\frac{\lambda n_{\rm Si}}{\alpha\,({\rm d}z/{\rm d}T)\,R_{\rm t}}, \tag{26}$$

where $Q_{\rm m}$ is the Q-factor of mechanical oscillation.

Before proceeding further, let us consider the case when the force acting on the beam is due to radiation pressure. Since the optical force in that case is simply twice the optical power divided by the speed of light, it is rather straightforward to repeat all the derivations with the main result being that, instead of $m\omega_0^2\alpha({\rm d}z/{\rm d}T)R_{\rm t}$, one should substitute $1/c$, where c is the speed of light. In place of the thermal time constant ($\tau_{\rm t}$) a cavity photon lifetime ($\tau_{\rm c} \sim Q_{\rm opt}\lambda/c$) should be used, resulting in

$$P_{\rm th,rad} \approx \frac{0.62}{Q_{\rm m}F^2}\frac{1+\omega^2\tau_{\rm c}^2}{\omega\tau_{\rm c}}\lambda n_{\rm Si} c m_{\rm eff}\omega^2 \approx \frac{0.62}{Q_{\rm m}Q_{\rm opt}F^2} m_{\rm eff} n_{\rm Si} c^2\omega, \tag{27}$$

consistent with [9]. Unless the cavity has an extraordinarily high $Q_{\rm opt.}$, $\omega\tau_{\rm c} \ll 1$ and the threshold of radiation pressure-driven oscillations is quite high. In contrast, in the case of

Table 1. Relevant parameters for the experimentally studied opto-mechanical oscillators.

Device	$\gamma/2\pi$ (Hz)	Q_m	F	T_{cav} (%)	z_1^{-1} (nm^{-1})	z_{sat} (nm)
1	5.54	1.89×10^4	140	4.7	1.6	12.9
2	3.98	2.79×10^4	380	4.1	7.7	4.8

a photothermal scheme one can design an optimum $\omega\tau_t \sim 1$ and achieve a low threshold in small cavities with a relatively modest Q_{opt}, as used in our experiments. At the same time, the radiation pressure-induced frequency shift term $(dz/dT)(T'_m/z_m)$ in equation (16), which according to (12) is proportional to $1/(1+\omega^2\tau_c^2)$, is much larger than the photo-thermally induced shift as is indeed observed in our experiments (figure 3).

4. Rate equation solution and comparison with experiment

To obtain input–output curves, it is convenient to define all the relevant energies and power as $u_{st} = U_{st}/U_{st,th}$, $u_m = U_m/U_{sat}$ and $p_{in} = P_{in}/P_{th}$ to obtain from (22) dimensionless laser equations identical to those in [15, 16]

$$\begin{aligned} \frac{du_{st}}{dt} &= \frac{1}{\tau_t}\left[p_{in}(1-u_m) - u_{st}\right], \\ \frac{du_m}{dt} &= \gamma\,(u_{st}-1)\,u_m + \gamma\frac{kT}{2U_{sat}}, \end{aligned} \tag{28}$$

where as we shall see below the noise term $kT/2U_{sat} \ll 1$. Note that (28) is obtained directly from (22) and is not limited to the weak vibration condition. Above threshold, the 'population inversion' gets clamped at a threshold $u_{st} = 1$ and the steady-state solution for the energy of mechanical oscillation can be found as $u_m = (p_{in}-1)/p_{in}$ with the term in the denominator indicating the phenomenon of 'gain compression' [20]. In real units we obtain for the output power dissipated by the mechanical beam and otherwise available to perform work $P_{out} = \gamma U_m = \eta_p\,(P_{in}/P_{th})^{-1}\,(P_{in} - P_{th})$ with the slope efficiency being equal to the pump efficiency modified by the gain compression term $(P_{in}/P_{th})^{-1}$. Using the second equation in (28) we can write for the linewidth:

$$\gamma_{eff} = \gamma\,(1-u_{st}) \approx \begin{cases} \gamma\,(1 - P_{in}/P_{th}), & P_{in} < P_{th}, \\ \gamma^2\frac{kT}{2P_{out}}, & P_{in} > P_{th}, \end{cases} \tag{29}$$

which is precisely the Schawlow–Townes expression for the linewidth [22] in which thermal noise energy kT replaced the quantum noise energy $h\nu$. Let us now estimate the relevant parameters for two cavities (device 1 and device 2) for which we have made 'lasing' measurements: the mechanical oscillation frequency for both devices is $\omega/2\pi = 101$ kHz; the other parameters are given in table 1. The thermal time constant has two components—the slower one equal to 162 μs (dominated by the microbridge) and the faster one equal to 3.0 μs (dominated by the DBR silicon slabs); only the fast component contributes appreciably to the resonance response with the term $\omega\tau_t/(1+\omega^2\tau_t^2)$ equal to 0.412 versus only 0.01 for the

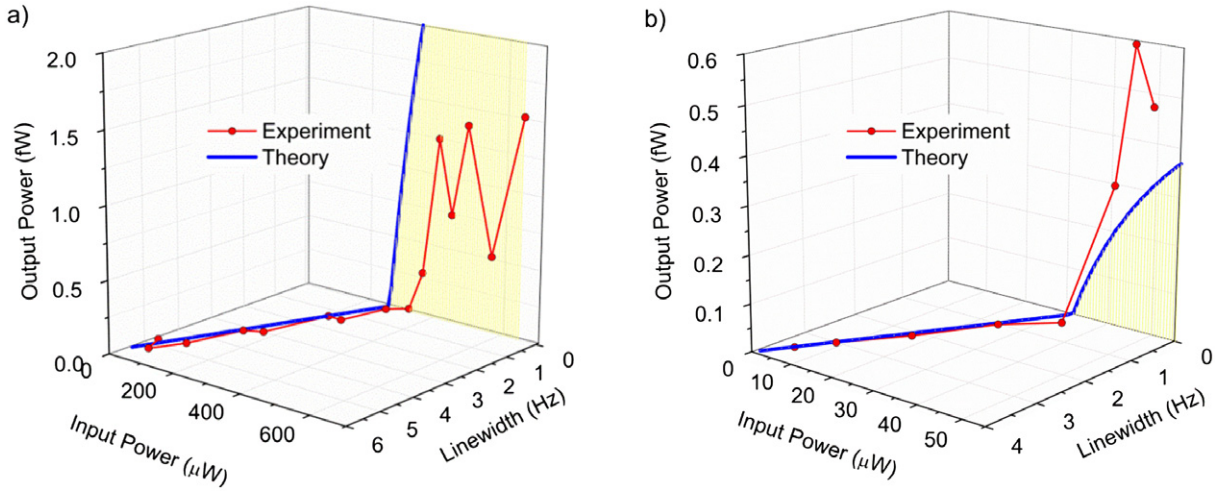

Figure 6. Comparison of the experimental (points) and the theoretical (lines) results for two devices: (a) device 1 output power and linewidth and (b) device 2 output power and linewidth. A few measured spectra corresponding to device 1 are shown in figure 3.

slow component [17]. Finally, the expansion term was estimated from a finite-element thermal-mechanical structural model to be $R_t\,(dz/dT) = 19.0 \times 10^3\,\mathrm{nm\,W^{-1}}$ [17].

To estimate the effective absorption in the DBR, we must take into account the fact that most of the absorption takes place in the first Si layer (facing the cavity) with thickness $d_{Si} = 653\,\mathrm{nm}$ and that the power inside that layer is reduced relative to the power bouncing inside the main Si spacer of the cavity. With the Si absorption coefficient equal to $\alpha_{Si} = 1.6\,\mathrm{cm^{-1}}$, we obtain $\alpha \approx 3.2 \times 10^{-5}$ and find the threshold powers for our two devices as 268 and 31.1 μW, respectively. Concerning the saturation power, we use the calculated result for the spring constant $K_{eff} = 2.75 \times 10^{-9}\,\mathrm{N\,nm^{-1}}$ to obtain saturation powers $P_{sat} = \gamma U_{sat}$ equal to 7.98 and 0.86 fW, respectively, with slope efficiencies of 3.1×10^{-11} and 3.6×10^{-11}, respectively.

The results of our calculation are plotted in figure 6, along with our experimental results for device 1 and device 2. Our instrument bandwidth is 1 Hz, which is deconvolved from our measured Lorentzian lineshapes. The experimental output powers are found by first converting our measured output laser oscillation amplitude into an oscillating displacement amplitude, which is then converted into a mechanical power. The experimentally observed threshold and linewidth are very well predicted by our theory in both devices. In the lower finesse device 1, the experiment shows earlier onset of saturation than theory, possibly due to the influence of the higher order terms in the Taylor expansion of the photo-thermal force. Also, while the average mechanical power follows the theoretical curve rather well, there are rather significant oscillations around the average power, which can also be associated with higher order nonlinear terms providing instability. In the higher finesse device 2 the observed output power is larger than predicted, which can be explained by the fact that in a higher Q cavity any small variation in laser wavelength can shift the position of the 'quiescent' point in figure 5 away from the one used to minimize threshold and effectively increase the saturation power. This accounts for some of the discrepancy between theory and experiment in both devices 1 and 2, although any wavelength shift will more significantly affect the threshold of the higher finesse device.

Furthermore, the coupling efficiency can differ between the two devices by a small amount due to the waveguide facet quality, for example. Also, even when they exist, the power variations in our device do not show a complicated, often multi-stable character observed in cantilevered designs [10, 21]. This can be explained by the fact that our cavity length is much shorter ($L_C = 3\,\mu$m) and we can keep the laser tuned close to a single quiescent point.

5. Microscopic picture

We now describe 'phonon lasing' on a quantum level. The majority of opto-mechanical oscillators in which phonon lasing has been demonstrated are driven by radiation pressure and can be explained in the framework of Raman lasers: a parametric process in which the stimulated decay of a higher frequency photon creates a quantum of mechanical oscillation and a lower frequency (Stokes) photon in the cavity. The Stokes shift is manifest in the fact that radiation pressure-driven phonon lasing always occurs when the pump photons are blue-shifted from the cavity resonance [7, 12]. Alternatively, one can visualize phonon lasing as a parametric oscillator in which pump photons are split into the low-frequency mechanical (acoustic) 'idler' phonon and a Stokes shifted 'signal' photon. But the situation is far more involved when the driving force is of a photo-thermal nature [5, 10] and the interaction is mediated by a sequence of processes taking place inside the medium (figures 4(a)–(c)). What is particularly intriguing is that depending on the particular design the 'lasing' can occur with either a blue- or a red-shifted pump (the latter being the case in our experiments), a fact that cannot be explained by conventional parametric and Raman-like processes.

However, the parametric explanation can be obtained on the microscopic level by noting that the thermal expansion driving the oscillating mechanical object is a consequence of the anharmonicity of the binding forces in the crystalline lattice. Both are described by the Grüneisen parameter [23]. It is precisely this anharmonicity that engenders the three-phonon quantum interactions, specifically the process in which a higher energy thermally excited acoustic phonon ω_p can split into two lower energy phonons. Here, one is the phonon of the mechanical oscillating mode with frequency ω_0 ('idler' phonon), while the other one is the thermal 'signal' phonon with frequency $\omega_p - \omega_0$ as shown in figure 7. The correspondence between the phonon anharmonicity and the second-order optical nonlinearity is well established and acoustic analogies of nonlinear optical process have been observed [24]. Hence, one can think of the oscillations as an 'acoustic parametric oscillator'. It is critical that the coherent buildup of idler oscillations takes place only if the 'pump' and 'signal' phonons remain locked in phase with each other for all phonon modes ω_p. Such a coherence is imposed by the fact that the light inside the optical cavity is modulated by the mechanical oscillations of one of the mirrors as $\cos(\omega_0 t)$. Hence, the power absorbed by the oscillating mirror and the temperature, i.e. the number of photo-generated phonons, is modulated as $\cos(\omega_0 t + \varphi)$ (figure 4(c)), and this modulation can be interpreted as interference between the phonons ω_p and phonon side bands $\omega_p \pm \omega_0$ whose phases are coherently related. When $\varphi = \pi/2$, (strong quadrature component in equation (12)), a buildup of coherent 'idler' oscillations will result in a manner similar to that of an optical parametric oscillator [25].

It is crucial to understand that there is no need for all the thermal phonons at different frequencies ω_p to be coherent among themselves. It is quite sufficient to have a relatively small fraction of these phonons separated by the idler frequency ω_0 to be locked in a phase relationship imposed by the oscillations of optical power. The energy of these pairs, U_{st}, can in principle be

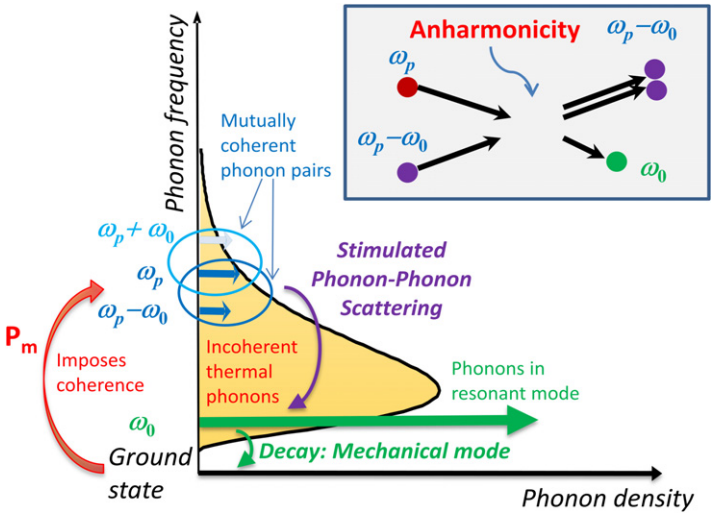

Figure 7. Coherent phonons at the difference frequency ω_0 that were generated in the resonant mechanical mode via anharmonicity.

transferred to the mechanical mode and it is this energy that plays the role of the energy stored at the upper level of the conventional laser.

Another analogy can be made with a different optical device: the opto-electronic microwave oscillator [26, 27]. This device is a source of microwave radiation in which the pump light is modulated by an electro-optic modulator driven by a microwave of frequency ω_0 obtained when the optical radiation is detected by a photodiode. The photodiode is a power detector (i.e. its response is quadratic in amplitude, similar to the second-order nonlinearity in parametric processes), and one can think of the photodetection as a process of down converting (heterodyning) of photons at laser frequency ('pump') and its side band ('signal') into the microwave 'idler'. A key feature of opto-electronic oscillators is that with a good microwave filter the linewidth of the generated microwaves can be much narrower than the linewidth of the pump laser, because each photon interacts only with its own sub-band shifted by ω_0 and the coherence of microwave radiation is not related to the coherence of the pump, but is determined by the quality factor of the microwave feedback loop and the output power. Similarly, the coherence of idler phonons in our experiments is determined only by the quality of mechanical resonance and the mechanical output power (equation (28)).

These analogies provide straightforward reasons for the low efficiency seen in our measurements. First of all, only a small fraction of all the phonons are the coherently locked ones. Secondly, in each three-phonon process the average pump photon of THz frequency creates a coherent phonon with less than a MHz frequency—hence the efficiency is low due to the Manley–Rowe limit in nonlinear optics [23]. Indeed, the frequency ω in the numerator of the expression for the efficiency is indicative of a Manley–Rowe relation.

6. Conclusions

We have derived a set of coupled phonon rate equations that describe above-threshold amplification and coherent self-oscillation in cavity opto-mechanical systems. These equations

have a form that is analogous to the laser rate equations, and consequently can be used to predict threshold pump powers, mechanical oscillation amplitudes and mechanical linewidths. The laser rate equation analogy also enables the identification of parameters such as effective opto-mechanical gain, saturation and slope efficiency. These equations are general for any opto-mechanical force, and we show excellent agreement with our experimental results obtained from photothermal pressure within an integrated Fabry–Perot microcavity coupled to a microbridge. Finally, we describe how this 'phonon-lasing' can be understood in terms of parametric amplification resulting from second-order nonlinear mixing between coherent phonons. We believe that the ultra-low mechanical linewidth that results from this coherent self-oscillation is of interest for sensing applications, in which a large mechanical Q-factor leads to enhanced sensing resolution, or microwave photonics in which an extremely narrow linewidth and low phase noise optical signals are required.

References

[1] Kippenberg T J and Vahala K J 2008 *Science* **321** 1172–6
[2] Favero I and Karrai K 2009 Optomechanics of deformable optical cavities *Nature Photon.* **3** 201–5
[3] Marqardt F and Girvin S M 2009 Optomechanics *Physics* **2** 40
[4] Armani D K, Kippenberg T J, Spillane S M and Vahala K J 2003 *Nature* **421** 925
[5] Metzger C H and Karrai K 2004 *Nature* **432** 1002–5
[6] Gigan S, Böhm H R, Paternostro M, Blaser F, Langer G, Hertzberg J B, Schwab K C, Bäuerle D, Aspelmeyer M and Zeilinger A 2006 *Nature* **444** 67–70
[7] Arcizet O, Cohadon P-F, Briant T, Pinard M and Heidmann A 2006 *Nature* **444** 71–4
[8] Schliesser A, Del'Haye P, Nooshi N, Vahala K J and Kippenberg T J 2006 *Phys. Rev. Lett.* **97** 243905
[9] Kippenberg T J, Rokhsari H, Carmon T, Scherer A and Vahala K J 2005 *Phys. Rev. Lett.* **95** 033901
[10] Metzger C, Ludwig M, Neuenhahn C, Ortlieb A, Favero I, Karrai K and Marquardt F 2008 *Phys. Rev. Lett.* **101** 133903
[11] Vahala K, Hermann M, Knunz S, Batteiger V, Saathoff G, Hansch T W and Udem T 2009 *Nature Phys.* **5** 682
[12] Grudinin I S, Lee H, Painter O and Vahala K J 2010 *Phys Rev. Lett.* **104** 083901
[13] Chan J, Alegre T P M, Safavi-Naeini A H, Hill J T, Krause A, Groblacher S, Aspelmeyer M and Painter O 2011 *Nature* **478** 89
[14] Siegman A E 1986 *Lasers* (Sausalito, CA: University Science Books)
[15] Statz H and De Mars G 1960 *Quantum Electronics* ed C H Townes (New York: Columbia University Press) 530
[16] Kleinman D A 1964 *Bell Syst. Tech. J.* **43** 1505
[17] Pruessner M W, Stievater T H, Khurgin J B and Rabinovich W S 2011 *Opt. Express* **19** 21904
[18] Khurgin J B, Pruessner M W, Stievater T H and Rabinovich W S 2012 *Phys. Rev. Lett.* **108** 223904
[19] Vogel M, Mooser C, Karrai K and Warburton R J 2003 *Appl. Phys. Lett.* **83** 1337
[20] Johnson B C and Mooradian A 1986 *Appl. Phys. Lett.* **49** 1135
[21] Marqardt F, Harris J G E and Girvin S M 2006 *Phys. Rev. Lett.* **96** 103901
[22] Schawlow A L and Townes C H 1958 Infrared and optical masers *Phys. Rev.* **112** 1940
[23] Dugdale J S and MacDonald D K C 1953 *Phys. Rev.* **89** 832–4
[24] Daly B C, Norris T B, Chen J and Khurgin J B 2004 *Phys. Rev.* B **70** 214307
[25] Shen Y R 1984 *The Principles of Nonlinear Optics* (New York: Wiley) chapter 9
[26] Yao S and Maleki L 1996 *J. Opt. Soc. Am.* B **13** 1725–35
[27] Maleki L 2011 *Nature Photon.* **5** 728–30